Effects of the capping ligands, linkers and oxide surface in the electron injection mechanism of copper sulfide Quantum Dots sensitized solar cells.†

Javier Amaya Suárez,[a] Jose J. Plata,*[b] Antonio M. Márquez,[a] and Javier Fdez. Sanz[a]

Because of the different components that constitute a quantum dots solar cells, QDSCs, and the difficulty of experimentally isolate the effect of each of them on the adsorption spectra of the system, we have modeled different Cu_2S QDSCs models by means of DFT. A bottom-up approach can differentiate the effect of each component in the electronic structure and absorption spectra. First, Cu_2S QDs were built including a U parameter to effectively describe the localization of the electrons. The effect of the capping agents was addressed using ligands with different electron-donating/- withdrawing groups. The role of the linkers and their adsorption of the surface of the oxide were also examined. Finally, we proposed a main indirect electron injection mechanism based on the position of the peaks of the spectra.

1 Introduction

Nanostructured particles or quantum dots (QDs) are one of the candidates to further increase the availability and efficiency of third-generation solar cells.[1] The efficiency of QDs solar cells (QDSCs) has rapidly growth during the last years[2–4] putting them on par with the dye sensitized solar cells (DSSC) and the bulk heterojunction (BHJ) photovoltaic cells.[5,6] Moreover, they are easy to synthesize, which reduces the time and cost of production.[7–10] Their popularity is also due to their high photostability, and, most importantly, their absorption spectra can be tuned by simply changing their size and composition.[11,12]

CdSe and CdTe have been extensively used as QDs for this kind of solar cells.[9] However, they present a variety of concerns such as low abundance, high cost and toxicity.[13] Recently, copper chalcogenides based materials have been proposed as one of the most promising candidates to substitute CdSe and CdTe for large scale, low cost, and sustainable solar cells.[14] Copper sulfides, $Cu_{2-x}S$, have been used as very efficient counter electrodes in QDSCs.[15,16] However, they were also introduced as part of the sensitizers in QDSCs obtaining promising results,[17,18] or combined with organic dyes to increase the efficiency of solar cells.[19] Because of their unique optical and electrical properties, copper sulfides nanoparticles have also been reported as a good visible-light-driven photo-catalyst.[20]

Despite of the fact that copper sulfides QDs are potential candidates for substituting conventional QDSCs based on CdSe and CdTe QDs, the optimization process of these devices remains an arduous challenge. The different components that constitute the QDSC (the oxide, linkers, ligands, or the counter electrode) and the mechanisms that govern its performance should be deeply evaluated to improve the efficiency of these devices. For instance, the role of capping ligands have been studied to improve the photoluminescence efficiency of the device.[21] The impact of the ligands on the morphology, electronic structure, and optical response of CdSe QDs has also been reported theoretically by means of time-dependent DFT (TDDFT).[1,22,23] The role of the linker also seems to be extremely important in the electron transfer between the dots and the oxide.[24,25] Long carrier lifetimes have been measured for copper oxide and sulfide QDs.[26]

In this article, copper sulfide based QDSCs have been modelled using a bottom-up strategy. The gradual growth of the model let us evaluate the contribution of each component in the optical and electronic properties of the system using DFT. A systematic study of the effect of different capping ligands and linker was performed. This information is critical for the rational design of more efficient devices and elucidating the electron transfer mechanism involved in the process.

2 Computational details and model

Periodic Density Functional Theory (DFT) calculations were carried out using the VASP 5.3 code[27–29] using the projector-augmented wave method (PAW).[30,31] The energies were computed with the exchange-correlation functional proposed by

[a] Departamento de Química Física, Facultad de Química, Universidad de Sevilla, 41012 Sevilla, Spain.

[b] Department of Mechanical Engineering and Materials Science, Duke University, Durham, North Carolina 27708, USA. E-mail: jose.plata@duke.edu
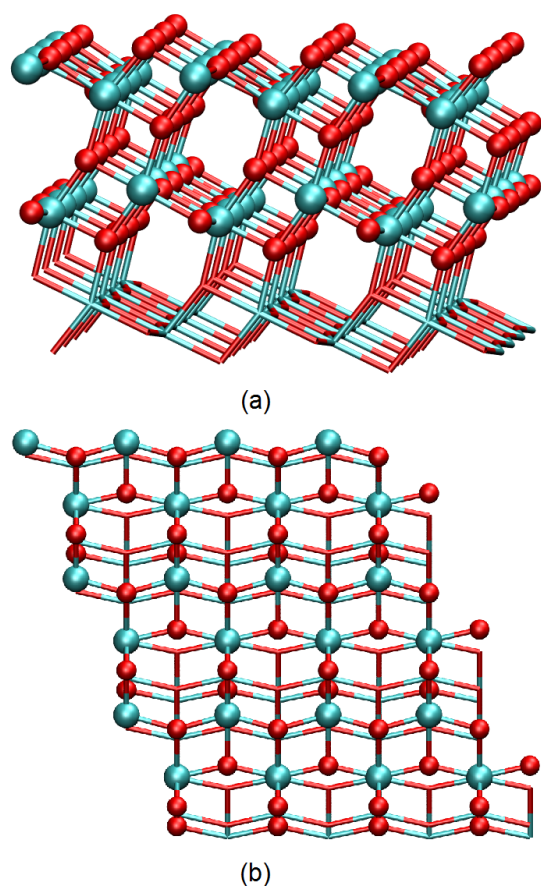
Fig. 1 (a) Side view and (b) top view of TiO_2-anatase (101) surface model. The atoms represented with balls correspond to the two upper relaxed layers. Colors: Ti, cyan; O, red.

Fig. 2 Cu_2S QDs geometries. Colors: Cu, ochre; S, yellow.

Perdew, Burke and Ernzerhof (PBE)[32] based on the generalized gradient approximation (GGA). It is well known that functionals incorporating some exact exchange are superior, in particular, in the estimation of the band gaps. However, their cost is still prohibitive for large systems. For this reason, we also incorporated an on-site Coulomb repulsion U term. The Hubbard U term was added to the plain PBE functional using the rotationally invariant approach proposed by Dudarev et al.,[33] in which the Coulomb U and exchange J parameters are combined into a single parameter U_{eff} = U - J. DFT+U calculations were performed, applying an U parameter on the Cu-3d and Ti-3d states respectively. Previous works have reported values of U_{eff} parameter for the Cu-3d states of 6.5 eV and 7.0 eV for CuO[34] and Cu_7S_4[35] respectively. Similarly, U_{eff} = 4.5 eV for Ti-3d levels have been previously used in for TiO_2.[36,37] All the calculations were undertaken using only the Γ point.[38] Forces on the ions were calculated through the Hellman-Feynman theorem, including the Harris-Foulkes correction to forces.[39] Iterative relaxation of the atomic positions and lattice parameters was stopped when the forces on the atoms were < 0.02 eV/Å. Optical spectra were obtained from the frequency-dependent dielectric function, $\varepsilon(\omega)$, as proposed by Gajdoš et al.[40] Isolated quantum dots were calculated using periodic cubic cells with at least 9 Å of vacuum
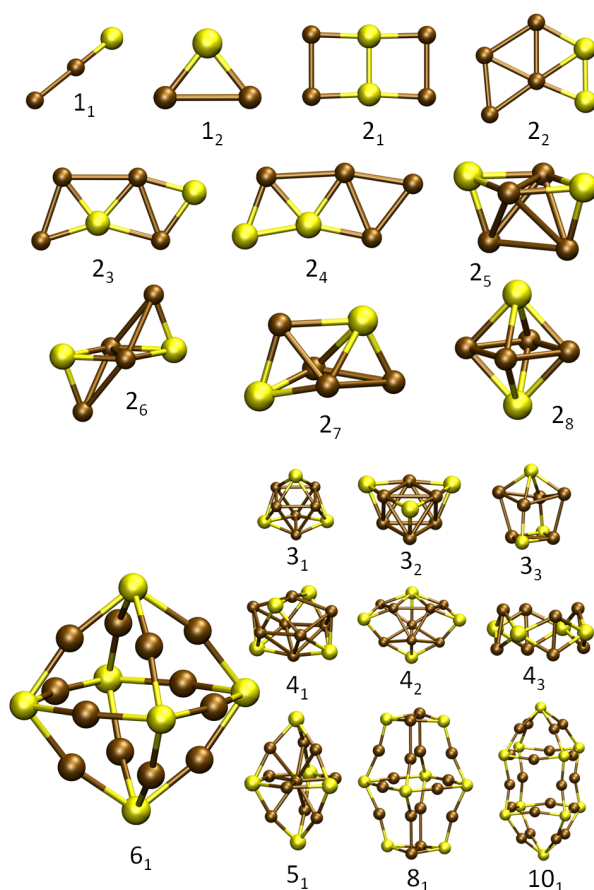
between the images. TiO_2-anatase (101) surface was modeled using a 4×3 slab surface with three-layer thickness (see Fig. 1). In this model, the two upper layers were relaxed while last layers were fixed to their bulk positions.

3 Results

3.1 Bare Cu_2S quantum dots

We have studied the relative stability, electronic properties and absorption spectra of different Cu_2S clusters that have been predicted for other authors[41] but using the methodological approach proposed in our previous work.[35] Clusters up to ten Cu_2S units, which are shown in Fig. 2, were considered in this article. Their relative stability, which is presented in Fig. 3, indicates that the energy per Cu_2S unit starts to converge around 6 units. For this reason, 6_1 cluster was chosen as QD model balancing the accuracy of the model and the computational cost. This cluster, with an O_h symmetry, contains 12 copper and 6 sulfur ions, all of them located at the surface creating an empty space in the center of the cluster. Its radius (3.14 Å) is lower than the reported value of the exciton Bohr radius for Cu_2S (30-50 Å), which is one of the requirements to be considered a QD.[42]

The electronic structure of the 6_1 cluster is predicted through the calculation of density of states (DOS), which is depicted in Fig. S1. Due to the non-periodic nature of the cluster and its size, the DOS of the QD is represented by localized states instead of
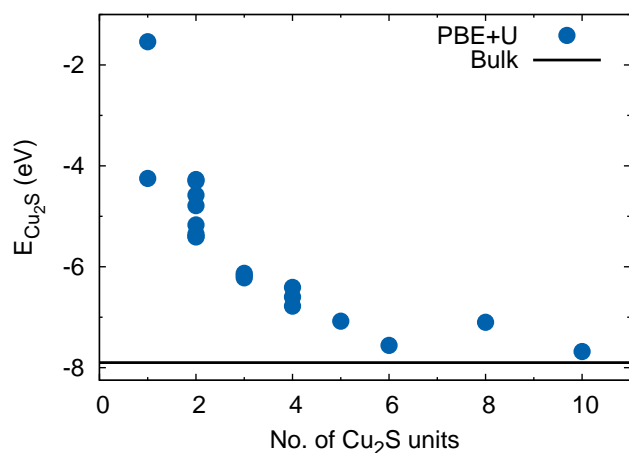
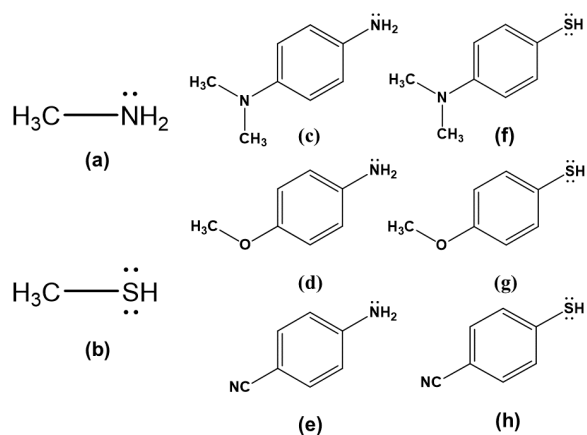**Fig. 3** Cu_2S QD energy per Cu_2S unit, E_{Cu_2S}, in eV.

Fig. 4 Structure of the ligands (a) Methanamine (MA), (b) Methanethiol (MT), (c) N1,N1-dimethylbenzene-1,4-diamine (DBD), (d) 4-methoxyamine (MAN), (e) 4-aminobenzonitrile (ABN), (f) 4-(dimethylamino)benzenethiol (DAB), (g) 4-methoxybenzenethiol (MBT) and (h) 4-mercaptobenzonitrile (MBN).

Table 1 Band gap, E_g, and first absorption peak values, E_{abs}, for the saturated model cluster with the different ligands. Energy values in eV.

Ligand	E_g	E_{abs}	Ligand	E_g	E_{abs}
MA	1.97	2.55	MT	2.20	2.52
DBD	2.15	2.44	DAB	2.18	2.44
MAN	2.20	2.55	MBT	2.25	2.63
ABN	2.27	2.70	MBN	2.21	2.32

wide bands. We obtained a band gap of 2.88 eV that is larger that the values for the bulk of any of the possible Cu_xS polymorphs (0.84-1.9 eV).[43–47] This phenomenon is produces by the destabilization of the unoccupied states or orbitals of undercoordinated atoms. The optical absorption spectrum follows the same trend that the DOS. with narrow peaks at energies above 3.9 eV (see Fig. S2).

3.2 Ligand-Cu_2S quantum dots models

The bare clusters are unstable and tend to agglomerate to reduce the surface energy of the system. In order to avoid this phenomenon, organic molecules are added to the solution to stabilize the QDs acting as ligands, which are coordinated to the copper cations. These molecules are usually organic molecules functionalized with amino and thiol groups. We have used eight ligands: methanamine (MA), methanethiol (MT), N1,N1-dimethylbenzene-1,4-diamine (DBD), 4-methoxyamine (MAN), 4-aminobenzonitrile (ABN), 4-(dimethylamino)benzenethiol (DAB), 4-methoxybenzenethiol (MBT), and 4-mercaptobenzonitrile (MBN) (see Fig. 4). Some of them are aromatic ligands with different functional groups to explore the effect of electron-donating/- withdrawing groups. For instance, -N(CH$_3$) and -OCH$_3$ groups present effects +I and +R respectively donating electronic density. However, groups such as -CN attract electronic density withdrawing electrons from the system. Besides the structural stabilization of the QD, the adsorption of the ligands produces other two main effects: i) a shift in the absorption spectra to lower or higher energies; ii) the stabilization of the charges or holes when an electron transfer takes place.

The ligand-QD systems were modeled adsorbing one ligand in each copper atom of the surface of the cluster. being the optimized structures for each of them depicted in Fig. 5. Different configurations were tested for the QDs coordinated with ligands that contain phenyl groups. In all the cases, the lowest relative energy was obtained when the phenyl rings are stacked in pairs maximizing the interaction of the π orbitals of the aromatic

groups.

We have computed the DOS of these ligand-QD systems and the values for their band gaps are included in the Table 1. The adsorption of the ligands produces a reduction of the band gap by 0.61-0.91 eV because of the stabilization of the conduction band due to the interaction with the thiol and amino groups. These results are also reflected in the optical spectra reducing considerably the position of the first peak in the spectra, E_{abs}, compared to the bare QD. In order to analyze the effect of the ligands we took as references the two aliphatic ligands: MA and MT. Both systems present similar values for E_{abs} being the QD-MT spectra slightly shifted to the red. A similar trend was observed for CdSe by Nadler *et al.* claiming that this red shift is due to the better hybridization of S orbitals with the CdSe unoccupied molecular orbitals[1].

The situation is more complex when aromatic ligands with substituents are introduced. As we mentioned, these substituents change the electronic properties of the QD-ligand system being electron-donating (EDG) or -withdrawing (EWG). If it is donating, the aromatic ligand stabilizes the photogenerated hole, and if it is withdrawing, the spectrum is usually shifted to longer wavelengths.[48] For instance, the -CN group in the ABN and MBN ligands is electron-withdrawing, which should result in a red shift of the spectrum.[49] That is the effect that we can observe for the QD-MBN system presenting a E_{abs} around 2.32 eV. However, the opposite effect is observed for ABN, obtaining a peak shifted to higher energies (E_{abs} = 2.70 eV). Similar results are obtained for
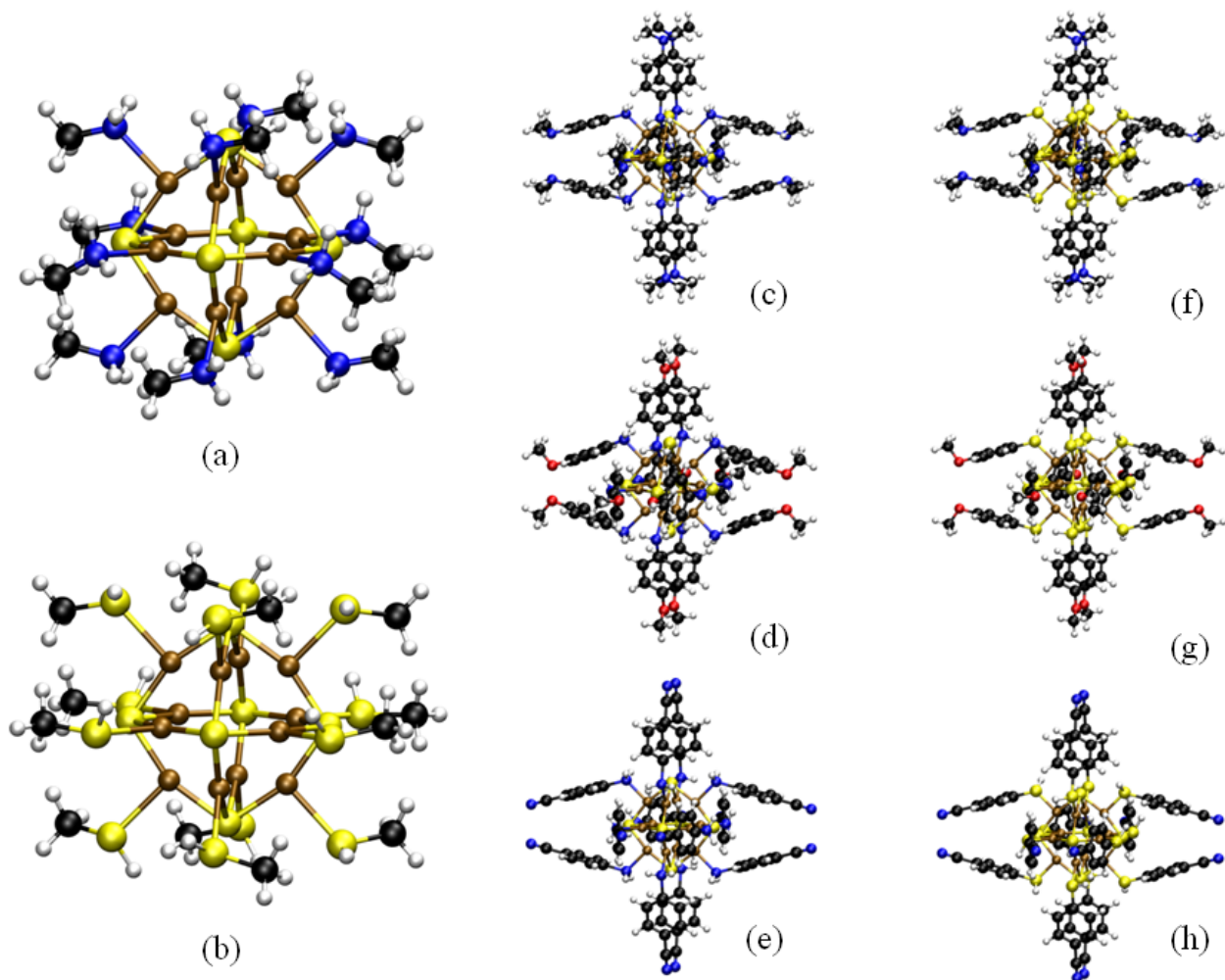
Fig. 5 Optimized geometries for QDs and (a) Methanamine (MA), (b) Methanethiol (MT), (c) N1,N1-dimethylbenzene-1,4-diamine (DBD), (d) 4-methoxyamine (MAN), (e) 4-aminobenzonitrile (ABN), (f) 4-(dimethylamino)benzenethiol (DAB), (g) 4-methoxybenzenethiol (MBT) and (h) 4-mercaptobenzonitrile (MBN).

the the system $(CdSe)_{13}(ABN)_6$,[1] which are explained by the less effective hybridization of the amine group orbitals with Cd compared to the dithiocarbamate functional group used by Frederick *et al.*[49] We have also functional groups that apparently do not modify the spectra compared to the aliphatic ligands. This is the case for the QD-MAN system whose E_{abs} (2.55 eV) matches perfectly with the value for the QD-MA system, which has been also reported for CdSe based QDs[1]. Finally, we observed that for electron donating substituents like the DBD and DAB ligands, there is a red shift of the spectra. This shift is due to the stabilization of the delocalized hole by the electron donating properties of the dimethylamino group.[48]

3.3 Linkers and adsorption on TiO$_2$ anatase (101)

The use of molecular linkers is a common approach for the sensitization of oxides with a band gap larger than 3 eV. The molecules used as linkers selectively anchor the QD to the surface of the oxide acting as a bridge between the donor and the acceptor respectively.[9,50–53] This bridge plays a crucial role in the kinetics of the electron transfer imposing a barrier potential ϕ that has to be overcome. Experimental studies have demonstrated that electron transfer is faster in linkers with aromatic structures instead of linear carbon chains.[25] However, to the best of our knowledge there is not any study about the influence of the chemical nature of the linkers in the absorption spectra of QDs sensitized oxides. We have studied four different linkers: cysteine (cys), histidine (his), 3-mercaptopropanoic acid (MPA) and 4-mercaptobenzoic acid (MBA). While MPA and MBA molecules were used to study the electron injection between CdSe and SnO$_2$,[25] aminoacides have been recently reported as a good linker between copper sulfide clusters and TiO$_2$ nanotubes.[17,54]

The first step to study the QD-linker-TiO$_2$ system is looking for the most stable adsorption sites of the linker on the oxide surface. The adsorption of carboxylic acids in anatase (101) has been extensively studied using DFT.[55–57] The carboxylic group is deprotonated and coordinated to two different Ti atoms on the surface. However, the situation is different for the amino acids, which can
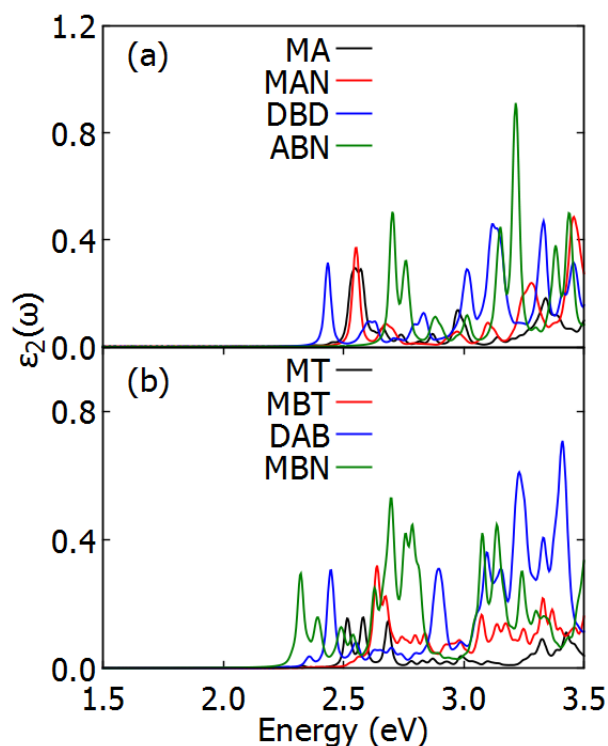
Fig. 6 Absorption spectra for QDs saturated with (a) amines and (b) thiols.

Table 2 First, second and third absorption energy, E_{abs}, values for QD-MA-Linker-TiO$_2$ with the different linkers. Energy values in eV.

Linker	1st	2nd	3rd
Cys	1.59	2.32	2.56
His	1.66	2.29	2.52
MPA	1.61	2.31	2.53
MBA	1.60	2.30	2.59

be adsorbed on the surface using two functional groups. Amino acids can be deprotonated and anchored to two surface by the two oxygen atoms ($d5$) as other carboxylic acids do or can be co-ordinated through the amine group and one of the oxygens without any deprotonation reaction ($m7$) (see Fig. 7) Both adsorption modes have been computed for the glycine being the $m7$ configuration just 0.048 eV more stable than the $d5$.[58] However, our results show that the cysteine and the histidine present the opposite behavior being the $d5$ configuration 0.15 and 0.2 eV more stable respectively than the $m7$ mode.

Finally we studied the the interaction of the Cu$_2$S QD with the linkers and the TiO$_2$ surface. MA molecules were selected as capping ligands to reduce the computational cost of the system (aprox. 330 atoms). The size of surface was modeled to create a monolayer of QDs over the surface (see Fig. 8 (a)) being the distance between images around 5 Å. The electronic structure of the system is not greatly modified by the linker. In all cases, the QD states overlap with the end of the valence band at TiO$_2$ and fill most of the gap (see Fig. 8 (b)). The occupation of the band gap by the QD states clearly affects the absorption spectra too. The zone of the visible spectra that it was empty for the bare
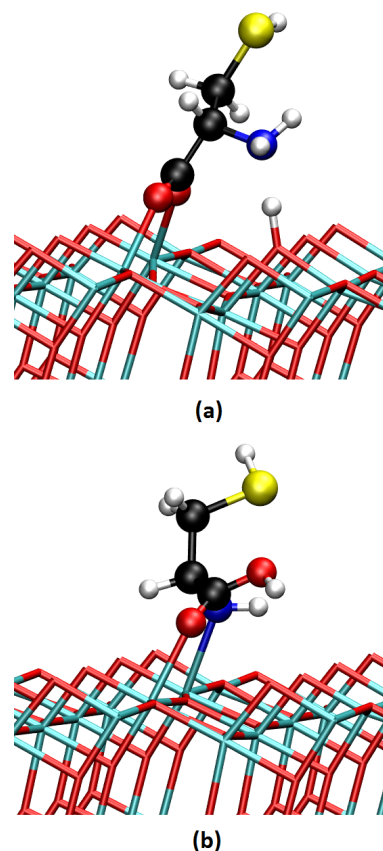

(a)

(b)

Fig. 7 Cysteine adsorption geometries onto anatase (a) d5 and (b) m7. Colors: Ti, cyan; O, red; C, black; H, white; N, blue; S, yellow.

TiO$_2$ surface is sensitized by the QDs (see Fig. 8 (c)). There are not big differences beyond small shifts (< 0.05 eV) in the peaks depending on the linker.

Finally, we can extract information about the injection mechanism comparing the peaks of the QDs with the ligands before and after been adsorbed on the surface. As a reference, we take the first intense peak of the QD-MA system at 2.55 eV in Fig. 6. An indirect injection mechanism between the QD and the surface will lead to very small or not variation of the feature of the main peaks of the QD spectra (see bottom scheme of the Fig. 8 (d)) while a direct mechanism will be linked to the appearance of peaks at lower energies (Fig. 8 (d)). Despite the different nature of both electron injection mechanisms, they coexist in real world situations. That is why we can find both kind of peaks in the absorption spectra of Fig. 8 (c). While there are small peaks at 1.6 eV and 2.3 eV, which should be representative of an indirect mechanism, the stronger peaks around 2.55 eV suggest that the main mechanism is indirect.

4 Conclusions

Because of the different components that constitute a QDSCs and the difficulty of experimentally isolate the effect of each of them on the adsorption spectra of the system, we have modelled dif-
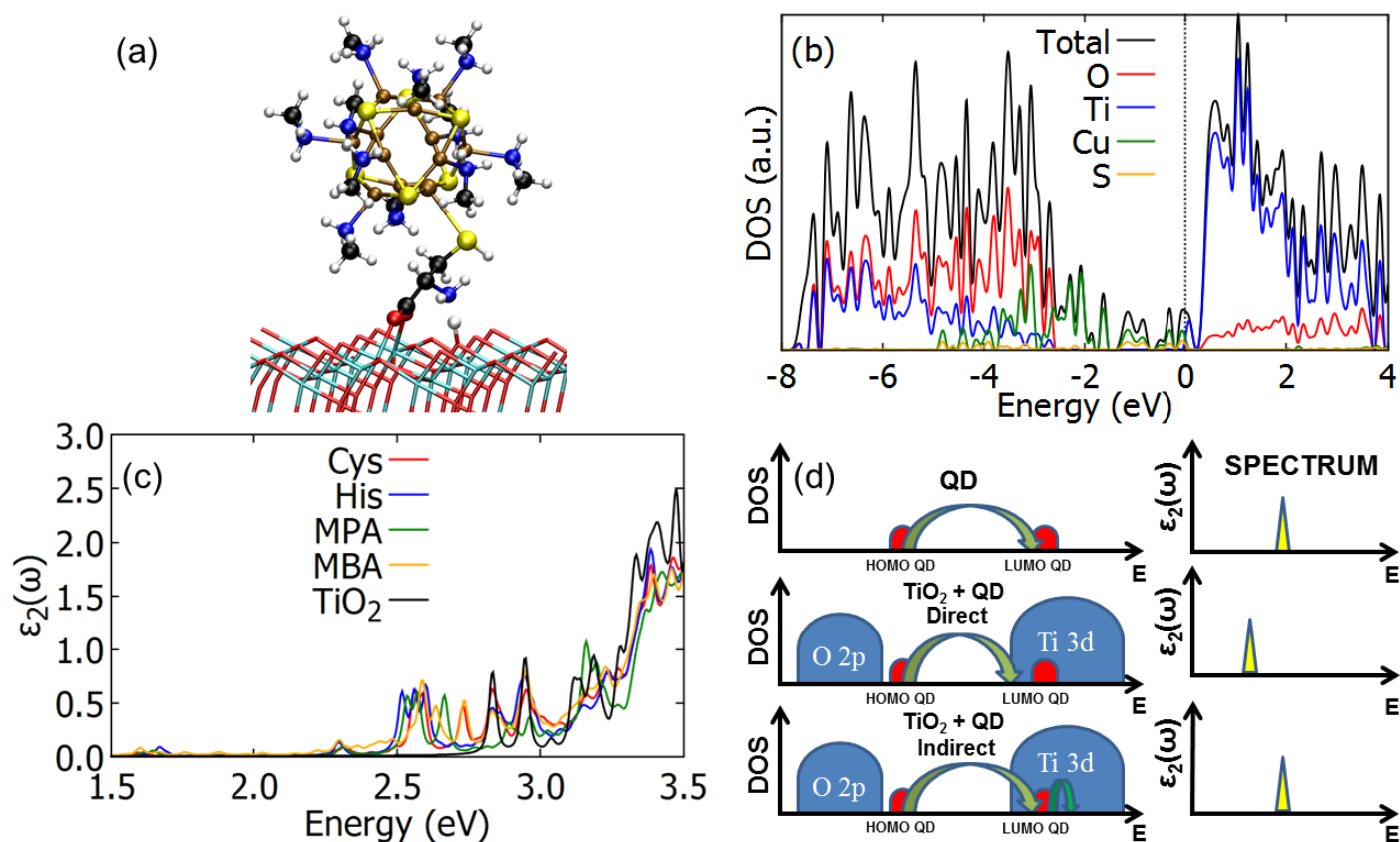
Fig. 8 (a) Optimized geometry for the QD-MA-Cys-TiO₂ system. Colors: Ti, cyan; O, red; C, black; H, white; N, blue; S, yellow; Cu, ochre. (b) DOS for the QD-MA-Cys-TiO₂ system. Fermi level is set at zero. (c) Absorption spectra for the QD-MA-Linker-TiO₂ with the different linkers. (d) Schematic diagram for different electron-injection mechanisms.

ferent Cu₂S based QDSCs models by means of DFT. A bottom-up approach let us differentiate the effect of each component in the electronic structure and absorption spectra. First, Cu₂S QDs were built including a U parameter to effectively describe the localization of the electrons. The effect of the capping agents was addressed using ligands with different electron-donating/- withdrawing groups. The role of the linkers and their adsorption of the surface of the oxide were also examined. Finally, we proposed a main indirect electron injection mechanism based on the position of the peaks of the spectra.

5 Acknowledgments*

References

1 R. Nadler and J. F. Sanz, *J. Phys. Chem. A*, 2015, **119**, 1218–1227.

2 A. Ip, S. Thon, S. Hoogland, O. Voznyy, D. Zhitomirsky, R. Debnath, L. Levina, L. Rollny, G. Carey, A. Fischer, K. Kemp, I. Kramer, Z. Ning, A. Labelle, K. Chou, A. Amassian and E. Sargent, *Nat. Nanotechnol.*, 2012, **7**, 577–582.

3 H.-S. Kim, C.-R. Lee, J.-H. Im, K.-B. Lee, T. Moehl, A. Marchioro, S.-J. Moon, R. Humphry-Baker, J.-H. Yum, J. Moser, M. Grätzel and N.-G. Park, *Sci. Rep.*, 2012, **2**, 591.

4 M. Lee, J. Teuscher, T. Miyasaka, T. Murakami and H. Snaith, *Science*, 2012, **338**, 643–647.

5 A. Yella, H.-W. Lee, H. N. Tsao, C. Yi, A. K. Chandiran, M. Nazeeruddin, E. W.-G. Diau, C.-Y. Yeh, S. M. Zakeeruddin and M. Grätzel, *Science*, 2011, **334**, 629–634.

6 F. He and L. Yu, *J. Phys. Chem. Lett.*, 2011, **2**, 3102–3113.

7 M. Islam and I. Herman, *Appl. Phys. Lett.*, 2002, **80**, 3823–3825.

8 P. Brown and P. V. Kamat, *J. Am. Chem. Soc.*, 2008, **130**, 8890–8891.

9 I. Robel, V. Subramanian, M. Kuno and P. V. Kamat, *J. Am. Chem. Soc.*, 2006, **128**, 2385–2393.

10 D. F. Watson, *J. Phys. Chem. Lett.*, 2010, **1**, 2299–2309.

11 P. K. Santra and P. V. Kamat, *J. Am. Chem. Soc.*, 2013, **135**, 877–885.

12 P. K. Santra and P. V. Kamat, *J. Am. Chem. Soc.*, 2012, **134**, 2508–2511.

13 Y. Zhao and C. Burda, *Energy Environ. Sci.*, 2012, **5**, 5564–5576.

14 C. Wadia, A. P. Alivisatos and D. M. Kammen, *Environ. Sci. Technol.*, 2009, **43**, 2072–2077.

15 C. S. Kim, S. H. Choi and J. H. Bang, *ACS Appl. Mater. Interfaces*, 2014, **6**, 22078–22087.

16 M. Ye, X. Wen, N. Zhang, W. Guo, X. Liu and C. Lin, *J. Mater. Chem. A*, 2015, **3**, 9595–9600.

17 C. Ratanatawanate, A. Bui, K. Vu and K. J. Balkus, *J. Phys. Chem. C*, 2011, **115**, 6175–6180.

18 S. Nelwamondo, M. Moloto, R. Krause and N. Moloto, *Materials Letters*, 2012, **75**, 161–164.

19 M. Mousavi-Kamazani, Z. Zarghami and M. Salavati-Niasari, *J. Phys. Chem. C*, 2016, **120**, 2096–2108.

20 S. Li, Z.-H. Ge, B.-P. Zhang, Y. Yao, H.-C. Wang, J. Yang, Y. Li, C. Gao and Y.-H. Lin, *Applied Surface Science*, 2016, **384**, 272–278.

21 G. K. Grandhi, A. M. and R. Viswanatha, *J. Phys. Chem. C*, 2016, **120**, 19785–19795.

22 S. Kilina, S. Ivanov and S. Tretiak, *J. Am. Chem. Soc.*, 2009, **131**, 7717–7726.

23 T. M. Inerbaev, A. E. Masunov, S. I. Khondaker, A. Dobrinescu, A.-V. Plamadă and Y. Kawazoe, *J. Chem. Phys.*, 2009, **131**, 044106.

24 I. Mora-Seró, S. Giménez, T. Moehl, F. Fabregat-Santiago, T. Lana-Villareal, R. Gómez and J. Bisquert, *Nanotechnology*, 2008, **19**, 424007.

25 H. Wang, E. R. McNellis, S. Kinge, M. Bonn and E. Cánovas, *Nano Letters*, 2013, **13**, 5311–5315.

26 Y. Lou, M. Yin, S. O'Brien and C. Burda, *J. Electrochem. Soc.*, 2005, **152**, G427–G431.

27 G. Kresse and J. Furthmüller, *Phys. Rev. B*, 1996, **54**, 11169–11186.

28 G. Kresse and J. Furthmüller, *Comput. Mater. Sci.*, 1996, **6**, 15–50.

29 G. Kresse and J. Hafner, *Phys. Rev. B*, 1993, **47**, 558–561.

30 G. Kresse and D. Joubert, *Phys. Rev. B*, 1999, **59**, 1758–1775.

31 P. Blöchl, *Phys. Rev. B*, 1994, **50**, 17953–17979.

32 J. Perdew, K. Burke and M. Ernzerhof, *Phys. Rev. Lett.*, 1996, **77**, 3865–3868.

33 S. Dudarev, G. Botton, S. Savrasov, C. Humphreys and A. Sutton, *Phys. Rev. B*, 1998, **57**, 1505–1509.

34 M. Heinemann, B. Eifert and C. Heiliger, *Phys. Rev. B*, 2013, **87**,.

35 J. Amaya Suárez, J. J. Plata, A. M. Márquez and J. F. Sanz, *Theor. Chem. Acc.*, 2016, **135**, 70(1–8).

36 J. B. Park, J. Graciani, J. Evans, D. Stacchiola, S. Ma, P. Liu, A. Nambu, J. F. Sanz, J. Hrbek and J. A. Rodriguez, *Proc. Natl. Acad. Sci.*, 2009, **106**, 4975–4980.

37 J. J. Plata, V. Collico, A. M. Márquez and J. F. Sanz, *J. Phys. Chem. C*, 2011, **115**, 2819–2825.

38 H. Monkhorst and J. Pack, *Phys. Rev. B*, 1976, **13**, 5188–5192.

39 J. Harris, *Phys. Rev. B*, 1985, **31**, 1770–1779.

40 M. Gajdoš, K. Hummer, G. Kresse, J. Furthmüller and F. Bechstedt, *Phys. Rev. B*, 2006, **73**,.

41 S. Dehnen, A. Schäfer, R. Ahlrichs and D. Fenske, *Chem. Eur. J*, 1996, **2**, 429–435.

42 Y. Zhao, H. Pan, Y. Lou, X. Qiu, J. Zhu and C. Burda, *J. Am. Chem. Soc.*, 2009, **131**, 4253–4261.

43 Y. Wu, C. Wadia, W. Ma, B. Sadtler and A. P. Alivisatos, *Nano Lett.*, 2008, **8**, 2551–2555.

44 P. S. McLeod, L. D. Partain, D. E. Sawyer and T. M. Peterson, *Appl. phys. lett.*, 1984, **45**, 472–474.

45 S. Couve, L. Gouskov, L. Szepessy, J. Vedel and E. Castel, *Thin Solid Films*, 1973, **15**, 223 – 231.

46 M. T. S. Nair, L. Guerrero and P. K. Nair, *Semicond. Sci. Technol.*, 1998, **13**, 1164.

47 Q. Xu, B. Huang, Y. Zhao, Y. Yan, R. Noufi and S.-H. Wei, *Appl. phys. lett.*, 2012, **100**, 061906.

48 Y. Tan, S. Jin and R. J. Hamers, *J. Phys. Chem. C*, 2013, **117**, 313–320.

49 M. T. Frederick, V. A. Amin and E. A. Weiss, *J. Phys. Chem. Lett.*, 2013, **4**, 634–640.

50 R. S. Dibbell and D. F. Watson, *J. Phys. Chem. C*, 2009, **113**, 3139–3149.

51 R. S. Dibbell, D. G. Youker and D. F. Watson, *J. Phys. Chem. C*, 2009, **113**, 18643–18651.

52 B.-R. Hyun, A. C. Bartnik, L. Sun, T. Hanrath and F. W. Wise, *Nano Lett.*, 2011, **11**, 2126–2132.

53 D. M. Adams, L. Brus, C. E. D. Chidsey, S. Creager, C. Creutz, C. R. Kagan, P. V. Kamat, M. Lieberman, S. Lindsay, R. A. Marcus, R. M. Metzger, M. E. Michel-Beyerle, J. R. Miller, M. D. Newton, D. R. Rolison, O. Sankey, K. S. Schanze, J. Yardley and X. Zhu, *J. Phys. Chem. B*, 2003, **107**, 6668–6697.

54 J. T. Margraf, A. Ruland, V. Sgobba, D. M. Guldi and T. Clark, *Langmuir*, 2013, **29**, 2434–2438.

55 D. C. Grinter, M. Nicotra and G. Thornton, *J. Phys. Chem. C*, 2012, **116**, 11643–11651.

56 A. Thomas, M. Jackman, M. Wagstaffe, H. Radtke, K. Syres, J. Adell, A. Lévy and N. Martsinovich, *Langmuir*, 2014, **30**, 12306–12314.

57 A. Vittadini, A. Selloni, F. P. Rotzinger and M. Grätzel, *J. Phys. Chem. B*, 2000, **104**, 1300–1306.

58 D. Szieberth, A. Maria Ferrari and X. Dong, *Phys. Chem. Chem. Phys.*, 2010, **12**, 11033–11040.